Published in final edited form as:
J Orthop Res. 2011 April ; 29(4): 501–510. doi:10.1002/jor.21270.

Cartilage Viability and Catabolism in the Intact Porcine Knee Following Transarticular Impact Loading with and without Articular Fracture

Jonathon D. Backus, M.D., **Bridgette D. Furman, B.S.**, **Troy Swimmer, M.S.**, **Collin L. Kent**, **Amy L. McNulty, Ph.D.**, **Louis E. DeFrate, Ph.D.**, **Farshid Guilak, Ph.D.**, and **Steven A. Olson, M.D.**
Division of Orthopaedic Surgery Department of Surgery Duke University Medical Center Durham, NC, USA

Abstract

Posttraumatic arthritis commonly develops following articular fracture. The objective of this study was to develop a closed joint model of transarticular impact with and without creation of an articular fracture that maintains the physiologic environment during loading. Fresh intact porcine knees were preloaded and impacted at 294 J via a drop track. Osteochondral cores were obtained from the medial and lateral aspects of the femoral condyles and tibial plateau. Chondrocyte viability was assessed at days 0, 3 and 5 post-impact in sham, impacted nonfractured, and impacted fractured joints. Total matrix metalloproteinase (MMP) activity, aggrecanase (ADAMTS-4) activity, and sulfated glycosaminoglycan (S-GAG) release was measured in culture media from days 3 and 5 post-trauma. No differences were observed in chondrocyte viability of impacted nonfractured joints (95.9±6.9%) when compared to sham joints (93.8±7.7%). In impacted fractured joints, viability of the fractured edge was 40.5±27.6% and significantly lower than all other sites, including cartilage adjacent to the fractured edge ($p<0.001$). MMP and aggrecanase activity and S-GAG release were significantly increased in specimens from the fractured edge. This study showed that joint impact resulting in articular fracture significantly decreased chondrocyte viability, increased production of MMPs and aggrecanases, and enhanced S-GAG release, whereas the same level of impact without fracture did not cause such changes.

Keywords

cartilage; posttraumatic arthritis; trauma; chondrocyte viability; intra-articular fracture

Introduction

Posttraumatic arthritis (PTA) is an important subset of osteoarthritis (OA) caused by injurious loading to a synovial joint, including meniscal, ligamentous, or joint capsule tears, joint dislocations, and most commonly and predictably, intraarticular fractures.[1] Furthermore, PTA affects a younger patient population, accounting for nearly 12% of OA cases.[2, 3] In the case of intraarticular fractures, the main therapeutic intervention is surgical restoration of joint anatomy in an effort to maintain joint function and prevent the onset of PTA.[4] However, despite advances in surgical technique, this disease still persists in many

Corresponding author: Steven A. Olson, M.D. Duke University Medical Center Box 3389 Durham, NC 27710 Tel (919) 668-3000 Fax (919) 668-2933 olson016@mc.duke.edu .

individuals[3], suggesting that molecular and cellular events at the time of injury may be crucial to disease progression.[5]

Although the exact etiology of PTA is not fully understood, it is hypothesized that inflammation and chondrocyte death are key events in disease progression.[6-9] For example, the pro-inflammatory cytokines interleukin 1 (IL-1), interleukin 6 (IL-6), and tumor necrosis factor alpha (TNF-α) are transiently elevated in the synovium and cartilage following joint injury[10]. These cytokines are believed to contribute to cartilage degeneration in OA through the activation of catabolic enzymes, such as matrix metalloproteinases (MMPs) and aggrecanases[11], leading to the breakdown and release of matrix fragments into the joint following injury.[12-16] Chondrocyte necrosis and apoptosis have also been observed following trauma, and these events are associated with cartilage damage and degeneration.[17, 18] It has been proposed that with decreased chondrocyte viability, the extracellular matrix cannot be maintained, leading to progressive cartilage degeneration.[17, 18] Moreover, it has been suggested that IL-1 and TNF-α may be initiating factors in chondrocyte apoptosis[19, 20]; however, the exact link between inflammation and cell death has not been fully elucidated.

Many of the findings linking injurious loading to chondrocyte death are based on *in vitro* explant models[19, 21, 22], *in vivo* animal models where a segment of an intact joint surface is impacted using standardized indenters[23, 24], or clinical studies.[17, 18, 25] Although these models have provided valuable information concerning chondrocyte death following both physiologic and injurious mechanical loads, there is limited data on chondrocyte viability in a controlled, closed joint model of intraarticular fracture where articular cartilage impacts opposing cartilage. *In vitro* explant and *in vivo* open joint models are arguably different from the physiologic environment of a joint, and in clinical studies the magnitude of joint loading and mechanism of injury is often unknown. The objective of this study was to create a closed articular fracture model in freshly harvested porcine knee joints to examine the response of chondrocytes to controlled transarticular loading, with and without articular fracture. Specifically, we determined the differences in cell viability, ADAMTS-4 and MMP activity, and sulfated glycosaminoglycan (S-GAG) release between closed knees impacted with and without articular fracture. Because PTA occurs most consistently following intraarticular fracture, we hypothesized that chondrocyte death, protease activity, and S-GAG release will be upregulated in joints that sustain an intraarticular fracture versus those that receive a similar load and do not fracture.

Materials and Methods

Intraarticular Fracture Model

Fifteen cadaveric porcine knees were obtained from a local abattoir within 12 hours of death. The knees were harvested from 2-3 year old skeletally mature female pigs that weighed approximately 180 kg to 450 kg. With the knees in extension, the femur, tibia and fibula were cut perpendicular to the diaphysis 7 cm superior to the patella and 7 cm distal to the tibial tubercle. Using a scalpel, soft tissue including the periosteum was removed approximately 5 cm from each cut end, while leaving the synovial capsule intact. The femur and tibia were then potted into custom symmetrical aluminum fixtures with fiberglass reinforced resin and polymethyl-methacrylate (PMMA). A pre-load of approximately 155 kg was applied across each joint in extension with six parallel springs (3 placed anterior, 2 placed posterior, and 1 placed on the lateral side of the knee) (Figure 1A).

Twelve joints were subjected to a 294 J impact (30 kg dropped from 1 meter) via a drop track outfitted with a hemispherical indenter. Fluoroscopy and a t-square were used to mark the upper aluminum fixture such that the indenter would impact the joint at predetermined

points relative to the anatomy of the knee joint. A sagittal view was utilized that impact would occur on the posterior aspect of the articular surface of the knee. From the coronal view, one of two orientations was chosen: 1) the joints were aligned with the indenter applying a transarticular load just lateral to the lateral tibial spine such that no fracture was created during impact; or 2) the joints were aligned with the indenter applying a transarticular load over the proximal tibiofibular joint, resulting in a lateral tibial plateau fracture (Figure 1B).

Immediately following impact, the joints were opened using sterile technique, and three 6.35 mm diameter osteochondral cores were obtained perpendicular to the articular surface from four anatomic quadrants within the joint. Cores were harvested from the medial and lateral sides of the femoral condyles and tibial plateau. In knees that were fractured, cores were obtained in the lateral tibial plateau that included the fractured edge (Figure 2). In one impacted fractured knee, only a single core could be harvested that included the fractured edge. This sample was immediately processed at day 0, and subsequently no confocal images were recorded of the fractured edge at day 3 and day 5. Three non-impacted sham joints were left in the potting apparatus to represent the elapsed time between potting and application of load in the impacted joints. After approximately 1 hour, osteochondral cores were harvested in a similar fashion as the impacted joints.

Cores were washed for 1 hour two times at 37°C in Dulbecco's modified Eagle's medium (DMEM; Invitrogen, Carlsbad, CA) containing 1,000 units/ml of penicillin/streptomycin/fungizone (Invitrogen, Carlsbad, CA). At days 0, 3, and 5 post-trauma, one core from each anatomical quadrant of the knee was analyzed for chondrocyte viability via a Live/Dead Viability/Cytotoxicity kit (Invitrogen). Culture time of 0, 3 or 5 days for the three osteochondral cores taken from each joint quadrant was varied in order to account for possible differences in viability for a specific anatomical location within a joint quadrant. There was no statistical significant effect of anatomical location on chondrocyte viability.

Osteochondral cores analyzed at days 3 and 5 were cultured in DMEM containing 10% heat-inactivated fetal bovine serum (Hyclone, Logan, UT), 0.1 m*M* nonessential amino acids (Invitrogen), 10 m*M* HEPES buffer solution (Invitrogen), 100 units/ml of penicillin/streptomycin, and 37.5 μg/ml of L-ascorbic acid 2-phosphate (Sigma-Aldrich, St. Louis, MO) at 37°C and 5% CO_2. The medium was collected at days 3 and 5, and fresh medium was added at day 3 for those cores cultured until day 5.

Chondrocyte Viability of Osteochondral Cores Following Impact

To assess chondrocyte viability, osteochondral cores were evaluated with the Live/Dead Assay. At time of analysis, each osteochondral core was halved using a straight edged razor applied perpendicular to the articular surface (Figure 3). Samples were washed for 5 minutes in phosphate buffered saline (PBS; Mediatech, Herndon, VA), stained for 25 minutes at room temperature in the dark with 4 μ*M* ethidium homodimer and 4 μ*M* Calcein AM in PBS, and then washed 2 times for 3 minutes each in fresh PBS. Cores were oriented with the cut edge face down on a chambered cover glass. Osteochondral cores were visualized using confocal laser scanning microscopy with an objective of 10X and numerical aperture of 0.30 (LSM 510; Carl Zeiss Instruments, Thornwood, NY). The diameter of porcine chondrocytes is 7-15 μm[26]; therefore, the optical slice was set at 15μm in order to image a single cell layer. Images were taken ≥ 50 μm into the face of the sample to avoid cells that may have been damaged during cutting. Images were taken throughout the entire depth of the cartilage, including the osteochondral junction (Figure 4).

Image Analysis

Image analysis was performed on two regions of interest: a central region of the core, and if present, the fractured edge (Figure 3). These regions were then divided by cartilage zones, defined as the superficial, middle, deep, and osteochondral zones, as previously described (Figure 4A).[27-30] Zeiss LSM Image Browsing software was used to identify these zones. The superficial zone was defined as the first 100 μm of cartilage from the articular surface, and the middle zone included cartilage 200-300 μm from the articular surface. The deep zone was defined as the first 200 μm from the osteochondral tidemark, and the osteochondral junction was defined as a subset of the deep zone that included the first 100 μm of cartilage from the tidemark. In the central region, the width of each zone of interest was defined as 500 μm. In the samples that included the fractured edge, the first 100 μm from the edge and the next 100 μm from the edge were analyzed (Figure 4B).

Dead cells were defined as those that incorporated the ethidium homodimer into their nuclei and fluoresced red, and live cells were defined as those that catalyzed Calcein AM and fluoresced green. All images were converted to grayscale (Adobe Photoshop, San Jose, CA) for image analysis (Scion Image; Scion Inc., Frederick, MD). Images were first converted to binary, and global intensity thresholds were selected to identify live and dead cells. In images with an exceptional amount of background staining, horizontal and vertical streaks were subtracted, using a built-in algorithm to remove smooth continuous backgrounds. The cell count from each channel was used to determine percent viability for each cartilage zone [% Viability = 100 X (live cells/(live cells + dead cells)]. Statistical analysis was performed using a three-way analysis of variance (ANOVA) with time treated as a repeated measure with a Tukey's post-hoc test.

MMP and Aggrecanase Activity

MMP and aggrecanase activity were measured in media samples collected at day 3 (n=120) and day 5 (n=60). A previously described fluorescence-based assay was used to measure total specific MMP activity in the culture media.[31] The assay is most specific for MMP-13 but the peptide substrate can also be cleaved by MMP-1, MMP-2, MMP-3, and MMP-9.[32] The total MMP activity for each osteochondral core was calculated and normalized by the volume of cartilage and per 24 hours of culture time. Aggrecanase-1 (ADAMTS-4) activity was measured in the culture media using a commercially available fluorescent peptide (WAAG-3R, AnaSpec, San Jose, CA) at a concentration of 25 μM.[33] Activity was normalized by the volume of cartilage and per 24 hours of culture time. Data from both assays were expressed as the mean activity ± 1 SEM. Since the data was not normally distributed, statistical analysis was performed on log transformed data using a three-way analysis of variance (ANOVA) with a Tukey's post-hoc test.

S-GAG Release

Total sulfated glycosaminoglycan (S-GAG) release was measured in media collected at day 3 (n = 120) and day 5 (n = 60) using the 1,9-dimethylmethylene blue (DMB) assay.[34] Standards were prepared ranging from 0 to 100 μg/mL bovine trachea chondroitin-4-sulfate type A (Sigma-Aldrich) in control media. Thirty microliters of standards and samples and 125μL DMB per well were added in duplicate to a 96-well plate. Absorbance was read at 540 nm within 5 minutes of adding DMB. The total μg of S-GAG released from each sample was normalized by the volume of cartilage and per 24 hours of culture time. Statistical analysis was performed using the non-parametric Kruskal-Wallis analysis of variance (ANOVA) for multiple independent samples.

Results

Impact Results

The average impact load was 19042.3 N ± 7239.8 N for impacted non-fractured joints and 17582.2 N ± 5424.8 N for impacted fractured joints. No statistically significant differences in the loads for impacted non-fractured and impacted fractured knees were detected (t-test, p=0.79); however, in three impacted non-fractured joints and one impacted fractured joint, the upper limit of the load cell was measured. Fractured joints were classified as Orthopaedic Trauma Association[35] (OTA) type B1 (n=4), C1 (n=1), and C3 (n=1) lateral plateau fractures.

Chondrocyte Viability

The effect of time post-trauma on chondrocyte viability for all groups (sham, impacted non-fractured, and impacted fractured) was not statistically significant (data not shown; ANOVA, $p>0.05$). Therefore, viability data was presented as the average of all time points. The impacted fractured joints demonstrated the lowest chondrocyte viability compared to impacted non-fractured and sham joints, with proximity to the fracture being the most significant factor (Figure 5).

For both the medial and lateral femoral condyles (Figure 5A and 5B), there were no statistically significant differences in viability between groups for all cartilage zones. In the medial tibial plateau (Figure 5C), the impacted fractured joints were significantly less viable than the impacted non-fractured and sham joints within the superficial zone only (ANOVA, $p<0.004$), and no statistically significant differences in viability were found between groups in the middle, deep, or osteochondral cartilage zones.

The lateral tibial plateau demonstrated the greatest decrease in viability (Figure 5D). Within the superficial zone of the articular cartilage in the impacted fractured joints, the first 200 μm along the fractured edge was significantly less viable than the central region of the impacted fractured, impacted non-fractured, or sham groups (ANOVA, $p<0.0002$), whereas the impacted non-fractured and sham joints were not significantly different from each other. For the middle zone, only the first 100 μm from the fractured edge was significantly less viable than all other groups (ANOVA, $p<0.001$). Within the deep and osteochondral zones, chondrocyte viability of only the first 100 μm along the fractured edge was significantly less viable than the central region of the impacted fractured, impacted non-fractured, or sham groups (ANOVA, $p<0.04$), but not significantly different from the next 100 μm along the fractured edge.

Over all cartilage zones, there was an average 42% decrease in chondrocyte viability along the fractured edge in comparison to the lateral tibia of sham and impacted non-fractured joints (ANOVA, $p<0.001$). Moreover, when compared to the adjacent central region of lateral tibial cartilage, overall chondrocyte viability at the fractured edge decreased by an average of 36% (ANOVA, $p<0.001$). In the impacted non-fractured joints, only the surface cartilage zone was affected and demonstrated a 13% decrease in chondrocyte viability in comparison to sham joints that was not a statistically significant difference (ANOVA, $p>0.05$).

In comparing viability among the different cartilage zones, there were several significant trends observed for both the impacted non-fractured and impacted fractured joints. The surface zone had the lowest chondrocyte viability (ANOVA, $p<0.05$), and the middle zone had the highest chondrocyte viability (ANOVA, $p<0.02$).

MMP and Aggrecanase Activity

There was a statistically significant effect of group and location on total MMP activity (Figure 6) (ANOVA, $p=0.001$). The lateral tibial plateau for the impacted fractured joints (Figure 6D) had significantly greater total MMP activity compared to the impacted non-fractured group (ANOVA, $p=0.0001$). Other locations within the joint did not show a statistically significant difference between groups (ANOVA, $p>0.05$). Additionally, there was no statistically significant effect of time on total MMP activity ($p=0.13$). A similar pattern was observed for aggrecanase-1 activity (Figure 7). There was a statistically significant effect of group and location on aggrecanase-1 activity (ANOVA, $p=0.001$) with the lateral tibial plateau for the impacted fractured joints demonstrating significantly greater activity than the impacted non-fractured group (ANOVA, $p=0.0005$) (Figure 6D). Other locations within the joint did not show a statistically significant difference between groups (ANOVA, $p>0.05$). Overall, aggrecanase-1 activity increased between 3 days and 5 days post-trauma (ANOVA, $p<0.0001$).

S-GAG Release

There was a statistically significant effect of group and location on total S-GAG release (Figure 8). The lateral tibial plateau for the impacted fractured joints (Figure 8D) had significantly greater S-GAG release compared to the impacted non-fractured group at 3 days post-trauma ($p=0.002$), and compared to the sham group at 5 days post-trauma ($p=0.009$). No statistically significant difference in S-GAG release was observed for other locations within the joint. Additionally, there was no statistically significant effect of time since trauma on S-GAG release ($p>0.05$).

Discussion

This model offers a novel system to study the changes in articular cartilage in an intact joint surface that has undergone impact from the opposing cartilage via axial transarticular loading. In the clinical setting, a lateral tibial plateau fracture is often created with a valgus stress coupled with an axial load.[36] Our system was designed to simulate a physiologically relevant mechanism of injury with a valgus stress being provided by an extra mechanical spring placed on the lateral side of the knee. Moreover, varying the alignment of the indenter allowed us to control the type of joint injury, resulting in a reproducible system where applying similar axial loads to a knee resulted in two different types of injury. With a more medial alignment of the indenter, the load was distributed more uniformly and no fracture was created following axial transarticular loading. A more lateral alignment of the indenter resulted in an articular fracture of the tibial plateau following axial transarticular loading. The intended impact result was demonstrated to be successful in 74% of all knees (20/27 total joints).

The results of this study support the hypothesis that chondrocyte death, cartilage proteolytic enzyme activity, and S-GAG release are significantly upregulated in joints that sustain an articular fracture versus those that experienced similar loading but did not fracture. Transarticular loading, as demonstrated by impacted non-fractured joints, caused some chondrocyte death in the superficial zone of cartilage from the lateral tibia; however, the fraction of cell death was significantly less than along the fractured edge in impacted fractured joints. Additionally, MMP and ADAMTS-4 activities and S-GAG release were increased only in samples that contained a fractured edge in impacted fractured joints. These results suggest that intraarticular fracture may play a greater role in the induction of chondrocyte death and cartilage catabolism than impact alone.

MMPs and aggrecanases are proteolytic enzymes that demonstrate an ability to cleave a wide range of extracellular matrix (ECM) components, including collagens, cartilage oligomeric matrix protein (COMP), and proteoglycans, such as aggrecan. These proteases play an important role in normal cartilage homeostasis and remodeling of extracellular matrix, but have been implicated in the destruction of cartilage and reported to be upregulated following joint injury or supra-physiologic loading of cartilage.[12-15, 22] Our results demonstrate that the activity of both matrix-degrading enzymes was significantly increased, and S-GAG release was also increased with fracture but not due to impact alone. This upregulation of MMP and aggrecanase activity may contribute to the onset of PTA, and the greater S-GAG release could be evidence of matrix degradation following articular fracture. Other investigators have reported that *in vitro* cartilage wounding with a trephine alone did not increase aggrecanase activity[37], suggesting that a combination of impact and traumatic disruption of the articular surface is required for increased proteolytic activity. The upregulated MMPs and aggrecanases may accelerate the degradation of the extracellular matrix and ultimately the development of PTA.

Our results for chondrocyte death due to cartilage impaction without fracture show significantly lower levels of cell death as compared to previous studies that have examined the effects of direct impact of the cartilage surface with an indenter, either in an open joint or a tissue explant model[19, 21-24, 38-42]. In our model, the articular cartilage was subjected to a transarticular impact in an intact joint. Cartilage away from the fractured edge demonstrated only slightly less viability than that of impacted non-fractured and sham joints, despite similar loads between the impacted fractured and impacted non-fractured groups (Figures 6A). These findings suggest that the threshold of stress that causes chondrocyte death following acute impact injury is much higher in a closed whole joint model, as compared to an *in vitro* explant model. Previous studies have reported that loads exceeding 25 MPa cause chondrocyte death in human cartilage.[38] This conclusion was based on a study in which cadaveric patellar cartilage was impacted directly using a drop tower apparatus, and cell death was measured by scanning electron microscopy and autoradiography. Others have reported that chondrocyte death and rupture of the articular cartilage collagen fibril network occurs at 15-20 MPa in a bovine cartilage explant model.[39] However, Borrelli *et al*.[40] have shown that the stress threshold for cartilage disruption or degradation may be much higher in an *in vivo* impact model of the rabbit femoral condyle. Impact stresses of 55.5 ± 12.6 MPa showed no structural damage, proteoglycan or collagen breakdown, or cellular proliferation. A subsequent study using the same model system suggested that stresses as high as 112 MPa were necessary to induce cartilage changes consistent with PTA progression.[41]

Regardless of whether an articular fracture was created, transarticular loading appeared to cause the greatest cell death in the superficial cartilage zone in this model. This decrease in superficial zone viability is consistent with both *in vitro* explant models[39, 43, 44] and clinical studies of traumatic injury.[18] The mechanism of increased cell death in this zone has been hypothesized to be a result of increased tissue and cell strain at the cartilage surface under compression.[45-47] The mechanical properties of articular cartilage differ by zone with the superficial zone having a significantly lower compressive modulus than other cartilage zones.[6, 48, 49] Other theoretical models suggest that even if cartilage had homogenous mechanical properties throughout the tissue, the highest shear forces would be experienced at the articular surface and osteochondral junction.[50, 51] The middle zone of cartilage in this model appears to be less susceptible to chondrocyte death following traumatic injury than other zones, consistent with a previous clinical study of human osteochondral fragments removed after articular fracture.[18] More investigations are needed in order to better characterize the protective mechanical and biologic properties of this cartilage zone.

Chondrocyte density decreases with age and in some cases may correlate with the progression of osteoarthritis.[52] It has thus been hypothesized that a sudden and significant loss of chondrocyte viability may contribute to cartilage degeneration in PTA.[17, 24, 53] The mechanism(s) of chondrocyte death may involve a combination of both necrosis and apoptosis, but several studies have suggested that apoptosis accounts for a significant portion of cell death.[9, 17, 53, 54] In this study, we measured chondrocyte viability to be 40.5% ±27.6% at the first 100μm from the fractured edge immediately after impaction. We recognize that apoptosis may contribute to the measured cell death[55]; however, we found no significant effect of time following impact on chondrocyte viability in the sham, impacted non-fractured, and impacted fractured joints in the present study, suggesting that cell death in this model was primarily due to necrosis. In summary, this study introduces a novel closed joint transarticular loading model that can be used to reproducibly create articular fractures similar to clinically observed fractures described by the OTA classification system. Additionally, the joint is not opened to create an articular fracture, avoiding direct manipulation of the articular tissues. The model was developed to allow either cartilage impact with or without articular fracture. Our data demonstrate that fracture is much more important than impact alone with a similar transarticular load and results in decreased chondrocyte viability, increased cartilage degradative enzyme activity, and increased S-GAG release. This model may aid in discovering the link between cell death and acute inflammatory changes that occur within the cartilage following trauma. Inhibiting MMP or aggrecanase activity following injury may slow or arrest the enzymatic degradation of joint tissues and aid in repair. This model will allow for future studies of acute cellular responses of joint tissues, their effect on chondrocyte death, and possible pharmacologic interventions following joint trauma.

Acknowledgments

Funding: NIH Grants AR50245, AR48852, and AR55434. No financial conflicts of interest to disclose. The authors would like to acknowledge Dianne Little, DVM, PhD, Richard Glisson, BS, and Poston Pritchett, BS for their technical support and expertise.

References

1. Swiontkowski MF, Agel J, McAndrew MP, Burgess AR, MacKenzie EJ. Outcome validation of the AO/OTA fracture classification system. J Orthop Trauma. Nov; 2000 14(8):534–541. [PubMed: 11149498]
2. Brown TD, Johnston RC, Saltzman CL, Marsh JL, Buckwalter JA. Posttraumatic osteoarthritis: a first estimate of incidence, prevalence, and burden of disease. J Orthop Trauma. Nov-Dec; 2006 20(10):739–744. [PubMed: 17106388]
3. Dirschl DR, Marsh JL, Buckwalter JA, et al. Articular fractures. J Am Acad Orthop Surg. Nov-Dec; 2004 12(6):416–423. [PubMed: 15615507]
4. Olson SA, Marsh JL. Posttraumatic osteoarthritis. Clin Orthop Relat Res. Jun.2004 (423):2. [PubMed: 15232418]
5. Catalano LW 3rd, Cole RJ, Gelberman RH, Evanoff BA, Gilula LA, Borrelli J Jr. Displaced intra-articular fractures of the distal aspect of the radius. Long-term results in young adults after open reduction and internal fixation. J Bone Joint Surg Am. Sep; 1997 79(9):1290–1302. [PubMed: 9314391]
6. Chen CT, Burton-Wurster N, Borden C, Hueffer K, Bloom SE, Lust G. Chondrocyte necrosis and apoptosis in impact damaged articular cartilage. J Orthop Res. Jul; 2001 19(4):703–711. [PubMed: 11518282]
7. Guilak F, Fermor B, Keefe FJ, et al. The role of biomechanics and inflammation in cartilage injury and repair. Clin Orthop Relat Res. Jun.2004 (423):17–26. [PubMed: 15232421]
8. Furman BD, Olson SA, Guilak F. The development of posttraumatic arthritis after articular fracture. J Orthop Trauma. Nov-Dec; 2006 20(10):719–725. [PubMed: 17106385]

9. Borrelli J Jr. Chondrocyte apoptosis and posttraumatic arthrosis. J Orthop Trauma. Nov-Dec; 2006 20(10):726–731. [PubMed: 17106386]
10. Lotz M. Cytokines in cartilage injury and repair. Clin Orthop Relat Res. Oct.2001 (391 Suppl):S108–115. [PubMed: 11603695]
11. Martel-Pelletier J, Alaaeddine N, Pelletier JP. Cytokines and their role in the pathophysiology of osteoarthritis. Front Biosci. Oct 15.1999 4:D694–703. [PubMed: 10525480]
12. Chubinskaya S, Kuettner KE, Cole AA. Expression of matrix metalloproteinases in normal and damaged articular cartilage from human knee and ankle joints. Lab Invest. Dec; 1999 79(12): 1669–1677. [PubMed: 10616215]
13. Kamekura S, Hoshi K, Shimoaka T, et al. Osteoarthritis development in novel experimental mouse models induced by knee joint instability. Osteoarthritis Cartilage. Jul; 2005 13(7):632–641. [PubMed: 15896985]
14. Lohmander LS, Hoerrner LA, Dahlberg L, Roos H, Bjornsson S, Lark MW. Stromelysin, tissue inhibitor of metalloproteinases and proteoglycan fragments in human knee joint fluid after injury. J Rheumatol. Aug; 1993 20(8):1362–1368. [PubMed: 8230020]
15. Sandy JD, Verscharen C. Analysis of aggrecan in human knee cartilage and synovial fluid indicates that aggrecanase (ADAMTS) activity is responsible for the catabolic turnover and loss of whole aggrecan whereas other protease activity is required for C-terminal processing in vivo. Biochem J. Sep 15; 2001 358(Pt 3):615–626. [PubMed: 11535123]
16. Lindhorst E, Vail TP, Guilak F, et al. Longitudinal characterization of synovial fluid biomarkers in the canine meniscectomy model of osteoarthritis. J Orthop Res. Mar; 2000 18(2):269–280. [PubMed: 10815829]
17. Kim HT, Lo MY, Pillarisetty R. Chondrocyte apoptosis following intraarticular fracture in humans. Osteoarthritis Cartilage. Sep; 2002 10(9):747–749. [PubMed: 12202127]
18. Hembree WC, Ward BD, Furman BD, et al. Viability and apoptosis of human chondrocytes in osteochondral fragments following joint trauma. J Bone Joint Surg Br. Oct; 2007 89(10):1388–1395. [PubMed: 17957084]
19. Kuhn K, Shikhman AR, Lotz M. Role of nitric oxide, reactive oxygen species, and p38 MAP kinase in the regulation of human chondrocyte apoptosis. J Cell Physiol. Dec; 2003 197(3):379–387. [PubMed: 14566967]
20. Aizawa T, Kon T, Einhorn TA, Gerstenfeld LC. Induction of apoptosis in chondrocytes by tumor necrosis factor-alpha. J Orthop Res. Sep; 2001 19(5):785–796. [PubMed: 11562122]
21. Chan PS, Schlueter AE, Coussens PM, Rosa GJ, Haut RC, Orth MW. Gene expression profile of mechanically impacted bovine articular cartilage explants. J Orthop Res. Sep; 2005 23(5):1146–1151. [PubMed: 16140194]
22. Lee JH, Fitzgerald JB, Dimicco MA, Grodzinsky AJ. Mechanical injury of cartilage explants causes specific time-dependent changes in chondrocyte gene expression. Arthritis Rheum. Aug; 2005 52(8):2386–2395. [PubMed: 16052587]
23. Borrelli J Jr. Tinsley K, Ricci WM, Burns M, Karl IE, Hotchkiss R. Induction of chondrocyte apoptosis following impact load. J Orthop Trauma. Oct; 2003 17(9):635–641. [PubMed: 14574191]
24. Duda GN, Eilers M, Loh L, Hoffman JE, Kaab M, Schaser K. Chondrocyte death precedes structural damage in blunt impact trauma. Clin Orthop Relat Res. Dec.2001 (393):302–309. [PubMed: 11764363]
25. Murray MM, Zurakowski D, Vrahas MS. The death of articular chondrocytes after intra-articular fracture in humans. J Trauma. Jan; 2004 56(1):128–131. [PubMed: 14749579]
26. Darling EM, Zauscher S, Guilak F. Viscoelastic properties of zonal articular chondrocytes measured by atomic force microscopy. Osteoarthritis Cartilage. Jun; 2006 14(6):571–579. [PubMed: 16478668]
27. Hwang WS, Li B, Jin LH, Ngo K, Schachar NS, Hughes GN. Collagen fibril structure of normal, aging, and osteoarthritic cartilage. J Pathol. Aug; 1992 167(4):425–433. [PubMed: 1403362]
28. Eggli PS, Hunziker EB, Schenk RK. Quantitation of structural features characterizing weight- and less-weight-bearing regions in articular cartilage: a stereological analysis of medial femoral condyles in young adult rabbits. Anat Rec. Nov; 1988 222(3):217–227. [PubMed: 3213972]

29. Hunziker EB, Michel M, Studer D. Ultrastructure of adult human articular cartilage matrix after cryotechnical processing. Microsc Res Tech. May 15; 1997 37(4):271–284. [PubMed: 9185150]
30. Jeffery AK, Blunn GW, Archer CW, Bentley G. Three-dimensional collagen architecture in bovine articular cartilage. J Bone Joint Surg Br. Sep; 1991 73(5):795–801. [PubMed: 1894669]
31. Wilusz RE, Weinberg JB, Guilak F, McNulty AL. Inhibition of integrative repair of the meniscus following acute exposure to interleukin-1 in vitro. J Orthop Res. Apr; 2008 26(4):504–512. [PubMed: 18050309]
32. Rasmussen FH, Yeung N, Kiefer L, et al. Use of a multiple-enzyme/multiple-reagent assay system to quantify activity levels in samples containing mixtures of matrix metalloproteinases. Biochemistry. Mar 23; 2004 43(11):2987–2995. [PubMed: 15023050]
33. Zhang Y, Xu J, Levin J, et al. Identification and characterization of 4-[[4-(2-butynyloxy)phenyl]sulfonyl]-N-hydroxy-2,2-dimethyl-(3S)thiomorpho linecarboxamide (TMI-1), a novel dual tumor necrosis factor-alpha-converting enzyme/matrix metalloprotease inhibitor for the treatment of rheumatoid arthritis. J Pharmacol Exp Ther. Apr; 2004 309(1):348–355. [PubMed: 14718605]
34. Farndale RW, Buttle DJ, Barrett AJ. Improved quantitation and discrimination of sulphated glycosaminoglycans by use of dimethylmethylene blue. Biochim Biophys Acta. Sep 4; 1986 883(2):173–177. [PubMed: 3091074]
35. Marsh JL, Slongo TF, Agel J, et al. Fracture and dislocation classification compendium - 2007: Orthopaedic Trauma Association classification, database and outcomes committee. J Orthop Trauma. Nov-Dec; 2007 21(10 Suppl):S1–133. [PubMed: 18277234]
36. Kennedy JC, Bailey WH. Experimental tibial-plateau fractures. Studies of the mechanism and a classification. J Bone Joint Surg Am. Dec; 1968 50(8):1522–1534. [PubMed: 5722848]
37. Tew SR, Kwan AP, Hann A, Thomson BM, Archer CW. The reactions of articular cartilage to experimental wounding: role of apoptosis. Arthritis Rheum. Jan; 2000 43(1):215–225. [PubMed: 10643718]
38. Repo RU, Finlay JB. Survival of articular cartilage after controlled impact. J Bone Joint Surg Am. Dec; 1977 59(8):1068–1076. [PubMed: 591538]
39. Torzilli PA, Grigiene R, Borrelli J Jr. Helfet DL. Effect of impact load on articular cartilage: cell metabolism and viability, and matrix water content. J Biomech Eng. Oct; 1999 121(5):433–441. [PubMed: 10529909]
40. Borrelli J Jr. Zhu Y, Burns M, Sandell L, Silva MJ. Cartilage tolerates single impact loads of as much as half the joint fracture threshold. Clin Orthop Relat Res. Sep.2004 (426):266–273. [PubMed: 15346084]
41. Borrelli J Jr. Silva MJ, Zaegel MA, Franz C, Sandell LJ. Single high-energy impact load causes posttraumatic OA in young rabbits via a decrease in cellular metabolism. J Orthop Res. Mar; 2009 27(3):347–352. [PubMed: 18924142]
42. Szczodry M, Coyle CH, Kramer SJ, Smolinski P, Chu CR. Progressive chondrocyte death after impact injury indicates a need for chondroprotective therapy. Am J Sports Med. Dec; 2009 37(12): 2318–2322. [PubMed: 19864505]
43. Milentijevic D, Torzilli PA. Influence of stress rate on water loss, matrix deformation and chondrocyte viability in impacted articular cartilage. J Biomech. Mar; 2005 38(3):493–502. [PubMed: 15652547]
44. Milentijevic D, Helfet DL, Torzilli PA. Influence of stress magnitude on water loss and chondrocyte viability in impacted articular cartilage. J Biomech Eng. Oct; 2003 125(5):594–601. [PubMed: 14618918]
45. Guilak F. Compression-induced changes in the shape and volume of the chondrocyte nucleus. J Biomech. Dec; 1995 28(12):1529–1541. [PubMed: 8666592]
46. Guilak F, Ratcliffe A, Mow VC. Chondrocyte deformation and local tissue strain in articular cartilage: a confocal microscopy study. J Orthop Res. May; 1995 13(3):410–421. [PubMed: 7602402]
47. Choi JB, Youn I, Cao L, et al. Zonal changes in the three-dimensional morphology of the chondron under compression: the relationship among cellular, pericellular, and extracellular deformation in articular cartilage. J Biomech. 2007; 40(12):2596–2603. [PubMed: 17397851]

48. Klein TJ, Chaudhry M, Bae WC, Sah RL. Depth-dependent biomechanical and biochemical properties of fetal, newborn, and tissue-engineered articular cartilage. J Biomech. 2007; 40(1): 182–190. [PubMed: 16387310]

49. Huang CY, Stankiewicz A, Ateshian GA, Mow VC. Anisotropy, inhomogeneity, and tension-compression nonlinearity of human glenohumeral cartilage in finite deformation. J Biomech. Apr; 2005 38(4):799–809. [PubMed: 15713301]

50. Eberhardt AW, Lewis JL, Keer LM. Normal contact of elastic spheres with two elastic layers as a model of joint articulation. J Biomech Eng. Nov; 1991 113(4):410–417. [PubMed: 1762438]

51. Ateshian GA, Wang H. A theoretical solution for the frictionless rolling contact of cylindrical biphasic articular cartilage layers. J Biomech. Nov; 1995 28(11):1341–1355. [PubMed: 8522547]

52. Vignon E, Arlot M, Vignon G. [The cellularity of fibrillated articular cartilage. A comparative study of age-related and osteoarthrotic cartilage lesions from the human femoral head]. Pathol Biol (Paris). Jan; 1977 25(1):29–32. [PubMed: 322033]

53. D'Lima DD, Hashimoto S, Chen PC, Lotz MK, Colwell CW Jr. Cartilage injury induces chondrocyte apoptosis. J Bone Joint Surg Am. 2001; 83-A(Suppl 2)(Pt 1):19–21. [PubMed: 11685837]

54. Hashimoto S, Takahashi K, Amiel D, Coutts RD, Lotz M. Chondrocyte apoptosis and nitric oxide production during experimentally induced osteoarthritis. Arthritis Rheum. Jul; 1998 41(7):1266–1274. [PubMed: 9663485]

55. D'Lima D, Hermida J, Hashimoto S, Colwell C, Lotz M. Caspase inhibitors reduce severity of cartilage lesions in experimental osteoarthritis. Arthritis Rheum. Jun; 2006 54(6):1814–1821. [PubMed: 16736522]

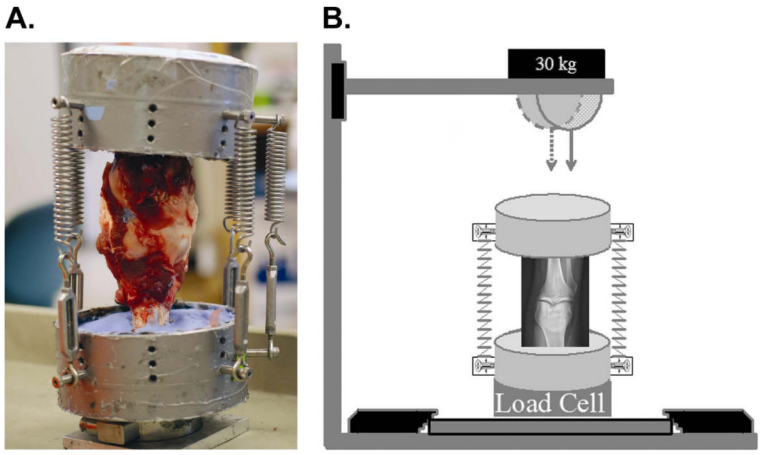

Figure 1.
Pre-load and impact alignment of closed porcine knee model. A. Posterior view of porcine knee potted in symmetrical aluminum fixtures and held in extension with 6 springs. B. The dashed arrow represents indenter alignment to impact a knee without fracture, and the solid arrow represents the alignment to impact a knee resulting in an intraarticular fracture.

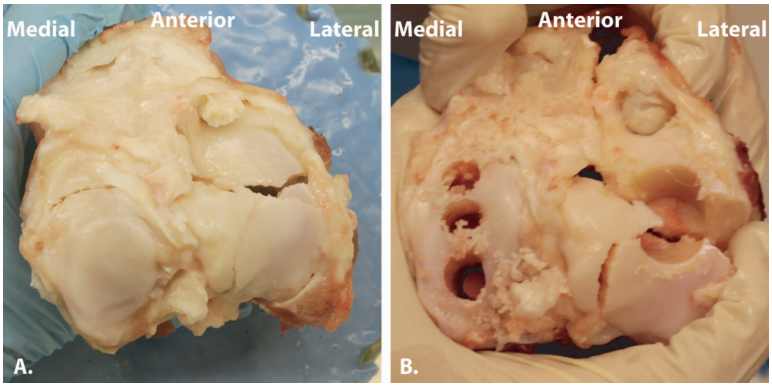

Figure 2.
Intraarticular fracture of porcine knee. A. Fractured tibial articular surface following transarticular loading. B. Fractured tibial articular surface demonstrating location of harvested osteochondral cores. Note that on the lateral tibial plateau, the fractured edge is included within the cores that were harvested.

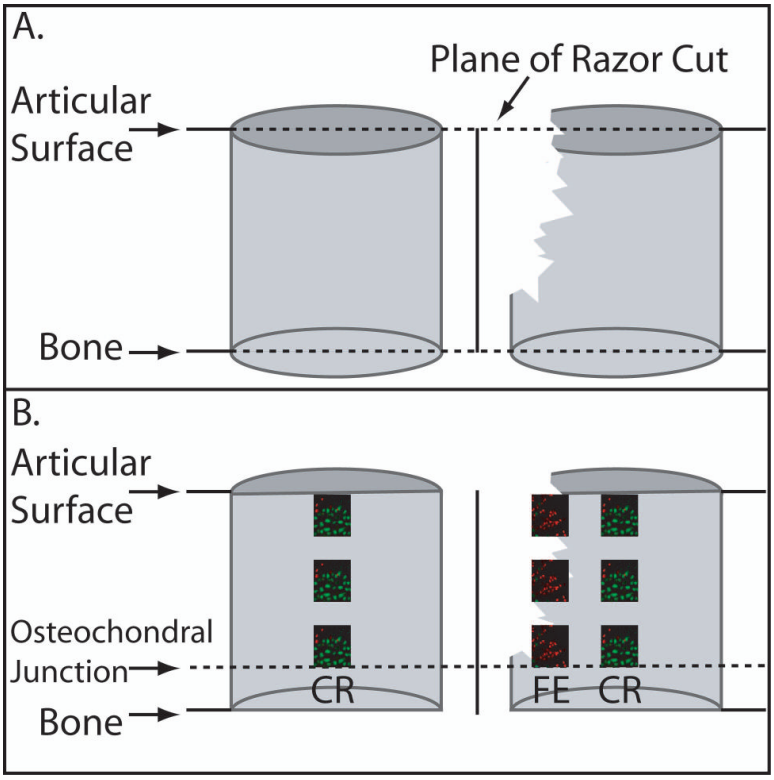

Figure 3.
Schematic of Osteochondral Core Processing. A. Demonstrates the perpendicular razor cut of the osteochondral cores with and without the fractured edge. B. Demonstrates the two regions of interest for confocal analysis of the live/dead assay. CR= Central Region. FE= Fractured Edge.

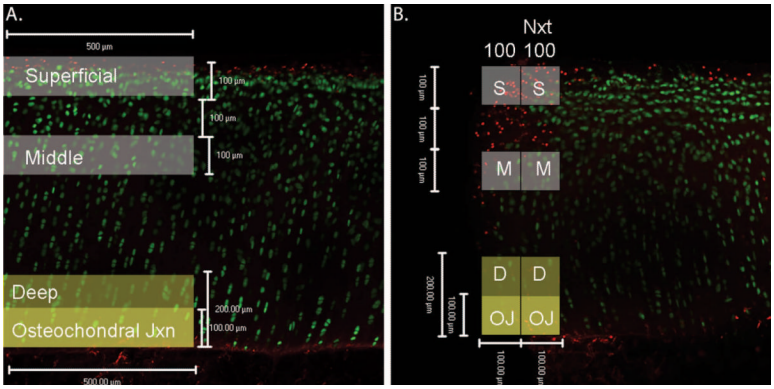

Figure 4.

Live/Dead Assay Confocal Microscope Images. Live cells stain green with Calcein AM stain and dead cells stain red with ethidium homodimer stain. A. Representative image of the central region. Shaded boxes represent the location and size of the cartilage zones that were analyzed. B. Representative image of the fractured edge region with the location and size of cartilage zones used for analyses shaded. The label '100' refers to the first 100 μm from the fractured edge and 'Nxt 100' refers to the region 100-200 μm away from the fractured edge.

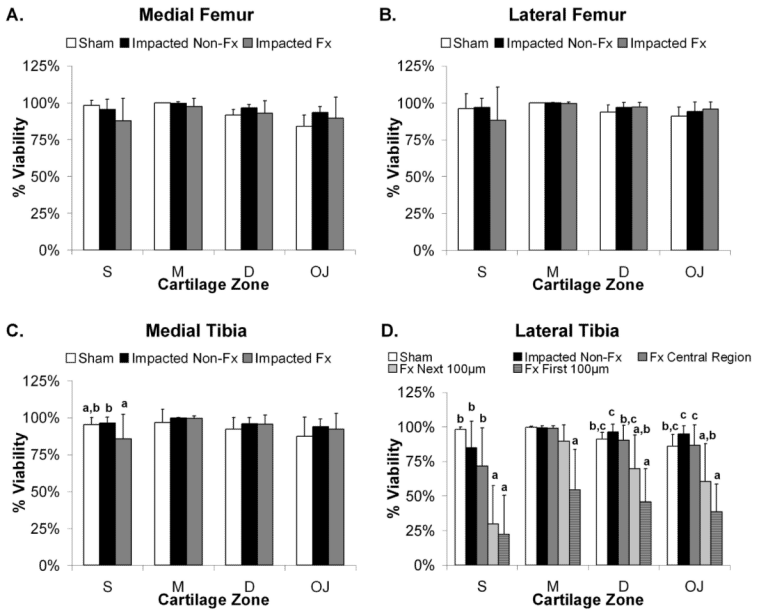

Figure 5.

Chondrocyte viability at the fractured edge is significantly less than the central regions across all impact results and joint quadrants. Bars show cell viability averaged over all time points and reported as mean percent viability + 1 standard deviation for: A. Medial femoral condyle, B. Lateral femoral condyle, C. Medial tibial plateau, and D. Lateral tibia plateau. Bars with different letters are significantly different from one another (ANOVA, $p<0.05$). S=Superficial Zone, M=Middle Zone, D=Deep Zone, and OJ=Osteochondral Junction.

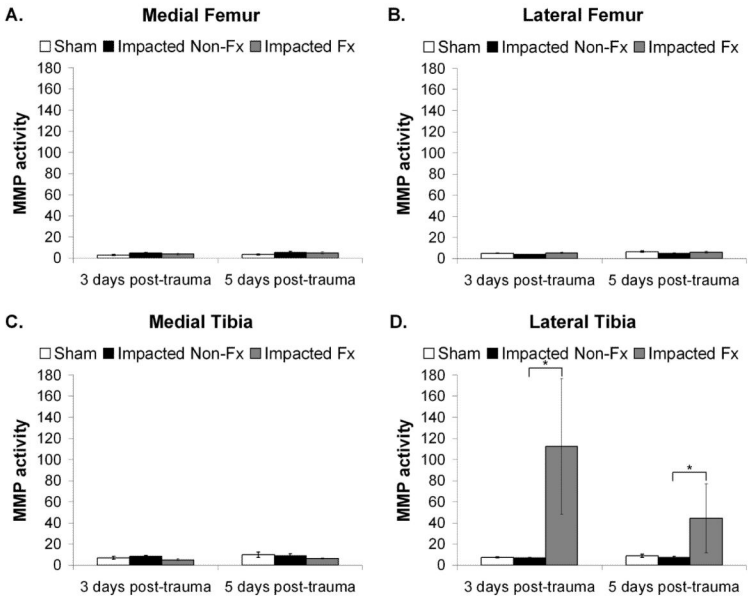

Figure 6.

MMP activity measured in fluorescent units and normalized to volume of cartilage and per 24 hrs of culture time. Data was reported as the mean activity ± 1 SEM for: A. Medial femoral condyle; B. Lateral femoral condyle; C. Medial aspect of the tibial plateau; and D. Lateral aspect of the tibial plateau. (ANOVA, *p = 0.0001).

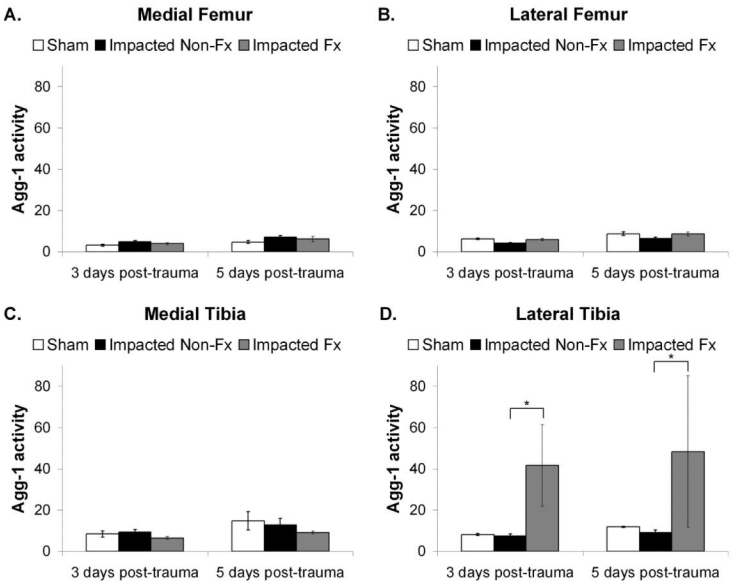

Figure 7.

Aggrecanase-1 (ADAMTS-4) activity measured in fluorescent units and normalized to volume of cartilage and per 24 hrs of culture time. Data was reported as the mean activity ± 1 SEM for: A. Medial femoral condyle; B. Lateral femoral condyle; C. Medial aspect of the tibial plateau; and D. Lateral aspect of the tibial plateau. (ANOVA, *p = 0.0005).

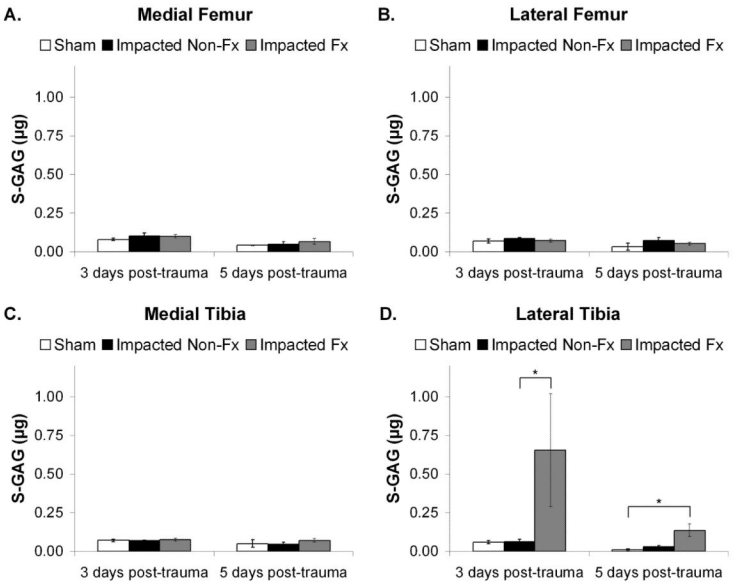

Figure 8.

Sulfated glycosaminoglycan (S-GAG) measured in µg and normalized to volume of cartilage and per 24 hrs of culture time. Data was reported as the mean activity ± 1 SEM for: A. Medial femoral condyle; B. Lateral femoral condyle; C. Medial aspect of the tibial plateau; and D. Lateral aspect of the tibial plateau. (Kruskal-Wallis, *$p < 0.002$).